

The South Atlantic and the Atlantic Meridional Overturning Circulation

Silvia L. Garzoli<sup>1</sup> and Ricardo Matano<sup>2</sup>

<sup>1</sup>Atlantic Oceanographic and Meteorological Laboratory, National Oceanic and  
Atmospheric Administration

<sup>2</sup>College of Oceanic and Atmospheric Sciences. Oregon State University

Revised version

April 2010

1 **Abstract**

2 This article discusses the contribution of the South Atlantic circulation to the variability  
3 of the Meridional Overturning Circulation (MOC). The South Atlantic connects the North  
4 Atlantic to the Indian and Pacific Oceans and as such it is the conduit through which the  
5 outflow of North Atlantic Deep Water (NADW) is compensated by a northward inflow of  
6 upper and intermediate waters. This circulation pattern in which cold waters flow  
7 poleward and warm waters equatorward generates a distinct heat flux that is directed  
8 from the poles towards the equator. Observations and models indicate that the South  
9 Atlantic is not just a passive conduit but that its circulation influences significantly the  
10 water mass structure of the Atlantic Meridional Overturning Circulation (AMOC). These  
11 transformations occur across the whole basin but are most intensified in regions of high  
12 mesoscale variability. Models and observations also show that the South Atlantic plays a  
13 significant role in the establishment of oceanic teleconnections. Anomalies generated in  
14 the Southern Ocean, for example, are transmitted through inter-ocean exchanges to the  
15 northern basins. These results highlight the need for sustained observations in the South  
16 Atlantic and Southern Ocean, which, in conjunction with modeling efforts, would  
17 improve the understanding of the processes necessary to formulate long term climate  
18 predictions.

19

19 **Introduction**

20 Two decades ago, discussions of greenhouse warming or the collapse of the global  
21 Meridional Overturning Circulation (MOC) were largely restricted to the academic elite.  
22 Nowadays, however, the same topics are the fodder of public debate. The general  
23 public's increased awareness of the physics of climate has been brought about partly by  
24 the mounting evidence that climate is indeed undergoing significant variability and  
25 change (e.g., data showing increases of global temperature during the last century and sea  
26 level rise), and partly by the predictions based upon model results about the consequences  
27 that such changes might have on our societies (IPCC, 2007). It is not always easy to  
28 separate fact from fiction, but the paleo-climate record indeed suggests that past  
29 shutdowns of the MOC triggered ice ages with dramatic decreases of the temperatures in  
30 western Europe and beyond (IPCC, 2007; Speich et al., 2010).

31

32 The perceived fragility of the climate system has prompted a flurry of new studies whose  
33 conclusions are, if not alarming, at least worrisome. Hansen et al. (2001) reported a 20%  
34 reduction in the overflow of deep waters through the Greenland–Scotland Ridge that  
35 feeds the densest portion of the MOC cell. Häkkinen and Rhines (2004) showed that the  
36 subpolar gyre of the North Atlantic has slowed appreciably during the last decade and  
37 suggested that a weakening of the MOC is underway. Bryden et al. (2005) argued that the  
38 strength of the MOC has decreased by more than 30% over the last five decades.  
39 Although none of these studies is conclusive as different models show different results,  
40 and the findings of Bryden et al., are based on just five hydrographic snapshots,  
41 nevertheless the robustness of the conclusions deserves the attention of the scientific

42 community.

43

44 Policymakers face the dilemma that, although the changes suggested by the above studies  
45 could be the heralded response of the oceans to global warming, they could just as well  
46 be a natural mode of oceanic variability. To separate anthropogenic from natural effects  
47 we need to substantially improve the existing observational system and foster the  
48 development of more complex models of the climate system. At present there is only one  
49 quasi-comprehensive monitoring system of the MOC in the northern North Atlantic: the  
50 RAPID/MOCHA array that, in conjunction with the observations of the warm, shallow  
51 limb in the Florida Current/Gulf Stream and of the Deep Western Boundary Current  
52 (DWBC) that started in the early 1980s off Florida (Baringer and Larsen, 2001; Meinen  
53 et al. 2006), provided the basin-wide integrated strength and vertical structure of the  
54 Atlantic Meridional Overturning Circulation (AMOC) at 26.5°N (Cunningham et al.,  
55 2007; Kanzow et al., 2007). Other attempts to monitor some of the components are  
56 located in other parts of the North Atlantic (e.g. the Denmark Straits overflow) and a  
57 small pilot effort recently started in the South Atlantic (Speich et al., 2010). They were  
58 designed to observe some of the important components of the AMOC that can in turn be  
59 used to verify and assimilate into models. (Østerhus et al., 2005; Srokosz, 2004, Baringer  
60 and Garzoli, 2007).

61

62 Given the complexity and the worldwide extent of the MOC it is obvious that even if  
63 these systems succeed in giving us a warning of potentially important changes of the  
64 MOC, the data collected by them are insufficient to determine the causality of such

65 changes, and they are therefore unable to predict further evolution of such changes. To do  
66 so, a more comprehensive view that takes into account the changes in the other basins is  
67 needed as well. To interpret the climate-related changes occurring in the North Atlantic,  
68 for example, we need to understand the variability of its contiguous basin, the South  
69 Atlantic; not only because its heat and salt fluxes are essential for the formation of the  
70 North Atlantic deep waters, but also because of its natural link with all the other major  
71 oceans. For the purposes of this study the South Atlantic is defined as the region between  
72 the tip of the Palmer Peninsula ( $60^{\circ}\text{S}$ ) and  $15^{\circ}\text{S}$  (the northern limit of the subtropical  
73 gyre) to encompass the subpolar and subtropical regions.

74

75 Although the contribution of the South Atlantic to the MOC was implicit in the early  
76 Meteor's observations (Wüst, 1935), which show a mean South Atlantic meridional  
77 circulation that exports heat in the "*wrong*" direction (e.g., from the south pole to the  
78 equator), there is still great uncertainty on the absolute magnitude of the South Atlantic  
79 interocean fluxes (see De Ruijter et al., 1999; Garzoli and Baringer, 2007). These  
80 uncertainties are compounded by the fact that the South Atlantic is not just a passive  
81 conduit for the transit of remotely formed water masses, but actively influences them  
82 through air–sea interactions, mixing, and subduction and advection processes. It is not  
83 sufficient, for example, to know the inflows at the Drake Passage and the Cape of Good  
84 Hope to determine the South Atlantic export of thermocline water to the North Atlantic.  
85 Indeed, it can be argued that since the South Atlantic circulation depends on the  
86 interoceanic fluxes and those in turn depend on the South Atlantic circulation, any  
87 attempt to determine one independently of the other leads to an ill-posed problem.

88

89 In this article an overview of the most outstanding characteristics of the South Atlantic  
90 circulation will be presented with emphasis on those aspects closely connected to the  
91 MOC. The goal is to illustrate the role that the South Atlantic plays in the MOC  
92 variability in order to highlight the importance of focusing some of the future research  
93 and monitoring efforts on the South Atlantic. Results of a numerical model and  
94 observations will be used to argue that the South Atlantic is not a passive ocean, that  
95 significant water mass transformations occur in the basin that affect the compensating  
96 flows that compose the AMOC, and that signals occurring in the adjacent oceans are  
97 transmitted through inter-ocean exchanges impacting its variability. An attempt will be  
98 made to demonstrate that, in addition to the already existent observations in the North  
99 Atlantic, monitoring the South Atlantic for inter-basin exchanges and the choke points  
100 that connect the basin with the Pacific and Indian Oceans will improve our understanding  
101 of these phenomena, facilitate the search for predictors, and lead to improved climate  
102 prediction models.

103

104

## 105 **2. Background**

106 The mean meridional structure of the South Atlantic circulation involves a deep  
107 southward flow of cold and salty North Atlantic Deep Water (NADW) along the eastern  
108 coast of South America, and compensating northward flows of surface, central, and  
109 intermediate waters. The South Atlantic connects with the Pacific and Indian Ocean  
110 providing the gateway by which the MOC connects with the rest of the globe. As such, a

111 significant exchange of water masses imported from the adjacent basins is to be expected.

112

113 The warm and salty water that spreads in the North Atlantic is cooled primarily by

114 evaporation, sinks to the deep ocean and forms the North Atlantic Deep Water (NADW)

115 (e.g. Gordon, 1986). Export of NADW to other ocean basins is compensated for by a net

116 northward flow through the South Atlantic and across the equator of surface, intermediate

117 and bottom water layers (Broecker, 1991; Schmitz, 1995; Speich et al. 2002). The

118 compensating northward flow is a mixture of warm and salty surface and central waters,

119 and cooler fresher Atlantic Intermediate Water (AAIW) (Figure 1). The surface water is

120 characterized by high salinity and is formed in the tropics/subtropics transition region by

121 subduction between 12 and 15 °S (Tomczack and Godfrey, 1994). Central water is

122 commonly subducted into the thermocline, and its formation in the South Atlantic occurs

123 at the confluence of the Brazil and Malvinas Currents (Gordon, 1989; Provost et al.,

124 1999) in the southwestern Atlantic with characteristics of Subtropical Mode Water at 16°

125 to 18°C. Also in the Southwestern Atlantic, the AAIW originates from a surface region of

126 the circumpolar layer, in particular north of the Drake Passage (Talley, 1996) and in the

127 Malvinas Current, a loop of the circumpolar current entering the South Atlantic. In the

128 eastern side of the basin, AAIW from the Indian Ocean enters the South Atlantic via the

129 Agulhas leakage.

130

131 This South Atlantic circulation pattern, in which warm waters flow towards the equator

132 and cold waters flow towards the pole results in an equatorward heat flux. This net

133 northward flow of properties is expected to be sensitive to the relative contributions of

134 the components of the returning flows originating in each one of the connecting oceans.  
135 The South Atlantic is the only basin extending to high latitudes in which the heat  
136 transport is equatorward. Although this distinct heat flux was recognized by the middle  
137 of the last century (Model, 1950), the sources for the upper waters are still in dispute. A  
138 portion of the South Atlantic upper waters is produced locally (see Stramma and England,  
139 1999, and references therein), but most of the South Atlantic upper waters are thought to  
140 originate in the Pacific and Indian Oceans. At issue are not only the relative importance  
141 of these sources but also the mechanisms of entrainment. Gordon (1986) proposed the  
142 warm path hypothesis, which postulates that the South Atlantic receives most of its upper  
143 waters from the Indian Ocean as eddies and filaments released at the retroflexion of the  
144 Agulhas Current and driven to the northwest by the Benguela and the Benguela Current  
145 extension. Rintoul (1991) proposed an alternative source, the cold-path, by which AAIW  
146 injected from the Pacific through the Drake Passage, is converted to surface water  
147 through air–sea interactions to become the main supply of South Atlantic upper waters.  
148 To reconcile the differences between these theories, Gordon et al. (1992) proposed a  
149 modification of the original warm path route by which the AAIW carried eastward by the  
150 South Atlantic Current is entrained into the Indian Ocean and recirculated by the Agulhas  
151 Current (Fig. 1).

152

153 It has been nearly two decades since the publication of Gordon’s and Rintoul’s influential  
154 articles, but there is still no consensus on the origins of the South Atlantic’s northward  
155 mass outflow (De Ruijter et al., 1999). Some of the studies that followed supported the  
156 cold-path theory (England et al., 1994; Macdonald, 1996; de las Heras and Schlitzer,



157 1999; Marchisiello et al., 1998; Sloyan and Rintoul, 2001; Nof, 1999; You, 2001), others  
158 the warm-path (Holfort and Siedler, 2001; Weijer et al., 2002; Donners and Drijfhout,  
159 2004; Speich et al., 2002), and still others postulated that both paths are important  
160 (Matano and Philander, 1993; Macdonald and Wunsch, 1996; Poole and Tomczack,  
161 1999). Donners and Drijfhout (2004) contested the studies supporting the cold-path  
162 hypothesis on the ground that their conclusions were biased by the method of analysis.  
163 Using the results of a global, eddy-permitting model they argued that the results of  
164 inverse calculations are hindered by their lack of spatial resolution. They showed that if  
165 the model results are analyzed within an Eulerian framework they also seem to suggest  
166 the dominance of the cold-path over the warm-path. However, if the model results are  
167 analyzed with a Lagrangian technique, which follows the trajectories of specific water  
168 masses, they show the dominance of the warm-path over the cold-path. Although these  
169 arguments are far from being conclusive, they clearly illustrate that the weakest link of  
170 existing estimates of the South Atlantic water mass balance is our lack of knowledge of  
171 the South Atlantic circulation itself. The uncertainty about the South Atlantic circulation  
172 also manifests itself in the estimates of the meridional heat transport, which vary from  
173 negative to positive values (e.g. Macdonald et al., 2001). This broad spread in the  
174 estimates reflects deficiencies in both the data available and in the methodology used for  
175 the calculation.

176

177 Since climate change studies assess the variability of the different components of the  
178 Earth system, it seems particularly worrisome that the gaps in our understanding of the  
179 South Atlantic variability are much larger than those of its mean circulation. There are

180 numerous studies on the mesoscale variability of the South Atlantic most energetic  
181 regions such as the Brazil/Malvinas Confluence (e.g. Olson et al., 1988; Gordon and  
182 Greengrove, 1989; Garzoli 1993; Matano et al., 1993) and the Agulhas retroflection (e.g.  
183 Lutjeharms and Gordon, 1987; Boebel et al., 2003), but very few on the low-frequency  
184 variability of the large-scale circulation. Venegas et al. (1997; 1998) and Palastanga et al.  
185 (2002) investigated the low-frequency variability of the South Atlantic's sea surface  
186 temperature (SST) from approximately 40 years of climatological data. They identified  
187 three low-frequency modes of variability with periods of about 14, 6, and 4 years that,  
188 according to their analyses, are associated with variations of sea-level pressure. Sterl and  
189 Hazeleger (2003) and Haarsma et al. (2005) added that these modes are generated by  
190 anomalous winds through turbulent heat fluxes, Ekman transport, and wind-induced  
191 mixing.

192

193 Although these studies are valuable contributions to our understanding of the climate  
194 variability over South America and Africa, it has been argued that SST anomalies don't  
195 necessarily reflect the variability of the oceanic circulation below the mixed layer. Witter  
196 and Gordon (1999) published an observational study of the low-frequency variability of  
197 the South Atlantic's thermocline circulation. Using four years of altimeter data they  
198 identified two dominant modes of sea surface height (SSH) variability. The first mode  
199 has a maximum in the eastern portion of the basin and indicated that the anti-cyclonic  
200 circulation in the subtropical gyre weakened from 1994 to 1996 and strengthened  
201 thereafter. They also observed a similar temporal signature in the zonal winds suggesting

202 a coupling between the oceanic and the atmospheric variability. The second mode was  
203 associated with interannual variations in the Brazil/Malvinas Confluence.

204

205 A recent study (Goni et al., 2010) analyzed the variability of the South Atlantic  
206 subtropical gyre using satellite derived SSH and SST anomalies and concluded that the  
207 interior of the gyre has expanded by ~40% of its total area. They also found that the  
208 mean dynamic height of the gyre had increased 3 cm per decade and hypothesized that  
209 this increase may be due to increased heat storage of the upper layer. Lumpkin and  
210 Garzoli (2010), through the analysis of a combination of surface drifters and altimetry  
211 found a southward shift of  $0.86 \pm 0.06$  degrees per decade in the confluence latitude of  
212 the Brazil and Malvinas Currents. A comparable trend is found in the latitude of the  
213 maximum wind stress curl averaged across the South Atlantic basin. This variation  
214 appears to be inversely related to long-term variations in SST anomaly in the Agulhas-  
215 Benguela pathway of the eastern South Atlantic subtropical basin. The time series of the  
216 bifurcation of the South Equatorial Current shows a trend of  $-0.23 \pm 0.06$  degrees per  
217 decade with an asymmetric growth of the subtropical gyre.

218

219 In summary, the South Atlantic is the main pathway of the compensating flows needed to  
220 maintain mass balance due to the export of NADW. This compensation is accompanied  
221 by a distinct northward heat transport. The strategic location of the South Atlantic raises  
222 the question of whether this basin is just a passive conduit for the passage of remotely  
223 formed water masses or whether its internal dynamics influences the MOC. To address  
224 this question in the following sections, the variability of the South Atlantic heat transport

225 (section 3) and its relation to internal dynamics (section 4) and inter-ocean exchanges  
226 (section 5) will be discussed.

227

228 For the purposes of this article we will discuss the results of the Parallel Ocean  
229 Circulation Model (POCM-4C), which is a global eddy-permitting numerical simulation  
230 that has been extensively compared with observations (e.g. Tokmakian and Challenor,  
231 1999; Baringer and Garzoli, 2007). To illustrate the realism of this simulation, in Figure 2  
232 we compare the mean circulation patterns derived by from this model with those inferred  
233 from the observations by Stramma and England (1999). The circulation patterns inferred  
234 from model and observations are remarkable similar. The left panel shows the  
235 observations and the right panel shows the model for the surface (top), intermediate  
236 (middle) and deep (lower) layers respectively. In both cases, the Agulhas Current intrudes  
237 in the southeast portion of the basin and retroflects at about  $20^{\circ}\text{E}$ . The Benguela Current  
238 and the Benguela Current extension form the eastern boundary current of the South  
239 Atlantic subtropical gyre (Peterson and Stramma, 1991; Richardson and Garzoli, 2003).  
240 The bifurcation of the South Equatorial Current is observed at about  $18^{\circ}\text{S}$  and the  
241 confluence of the Brazil and Malvinas at approximately  $38^{\circ}\text{S}$ , both in the model and the  
242 observations. The southern edge of the subtropical gyre is also located at  $45^{\circ}\text{S}$  in both  
243 cases. The AAIW (middle panel) shows a shift of the upper boundary of the gyre to the  
244 south and a recirculation cell in the western basin. The DWBC flows southward along the  
245 continental shelf of South America, breaks down into eddies at approximately  $18^{\circ}\text{S}$   
246 (Schott et al. 2005), and reconstitutes again south of  $27^{\circ}\text{S}$ .

247

### 248 **3. The South Atlantic's heat transport**

249 During WOCE, two zonal hydrographic sections confirmed that there is a net northward  
250 heat flux associated with the MOC (e.g. Ganachaud and Wunsch, 2003). Estimates of this  
251 heat flux in the North Atlantic range from 0.9 PW to 1.6 PW. The South Atlantic  
252 estimates are more uncertain than those in the North Atlantic. Within the subtropical  
253 region, the northward heat flux estimates range from negative values (-0.23 PW, de las  
254 Heras and Schlitzer, 1999) to almost 1 PW (0.94 PW, direct method, Saunderson and King  
255 1995; 0.88 PW, Inverse model Fu, 1981) where  $1\text{PW} = 10^{15}$  Watts. Differences in the  
256 estimates derived from observations may be a consequence of the different methods used  
257 to calculate the heat transport and the different database used. Heat transport differences  
258 between the models may be a consequence of the models' ability to reproduce the  
259 pathways of the intermediate water and to represent the variability of the boundary  
260 currents. However, large heat transport variability may be a real feature of the South  
261 Atlantic circulation due in part to the large meso-scale variability, particularly at the  
262 boundaries. Both margins are characterized as highly energetic and variable regions and  
263 therefore, natural variability cannot be ruled out. In order to understand the validity of the  
264 northward heat transport estimates, it is important to understand the mesoscale variability  
265 of the boundary currents. Having a clear understanding of the mesoscale variability is  
266 also valid for monitoring the MOC. Observations will be highly resolved in time and then  
267 used to filter out the mesoscale variability so that components that are only from the  
268 mesoscale are not attributed to MOC. However, mesoscale variability may be also due to  
269 real changes in the MOC. For example there is evidence that as Agulhas leakage  
270 diminishes, ring shedding also diminishes (Bjornsson et al., 2009). This would be a case

271 where the mesoscale variability may be due to real changes in MOC.

272

273 In a recent publication (Baringer and Garzoli, 2007), the product of the POCM model  
274 was analyzed to obtain the meridional heat transport across 30° and 35°S. Results from  
275 the POCM analysis (Fig 3) yielded to a mean heat transport at 30°S equal to  $0.55 \pm 0.24$   
276 PW, and  $0.6 \pm 0.27$  PW at 35°S. These results are in good agreement with observations at  
277 35°S of  $0.54 \text{ PW} \pm 0.11 \text{ PW}$  (Garzoli and Baringer, 2007). The time series of POCM heat  
278 transport are shown in Figure 3, top panel. The series show seasonal and interannual  
279 variability and a marked annual cycle. The existence of this annual cycle is not consistent  
280 with the observations to date. According to Garzoli and Baringer (2007), the Ekman  
281 component of the heat transport has a marked annual cycle that is opposite in phase from  
282 the geostrophic component of the heat transport. As a result, the total heat transport,  
283 which is defined as the sum of its components, shows a seasonal signal of smaller  
284 amplitude.

285

286 There is a close relationship between the South Atlantic heat transport and the strength of  
287 the AMOC. Analysis of hydrographic data collected along nominally 35°S (Dong et al.,  
288 2009) indicates that the northward heat transport variability is significantly correlated  
289 with the AMOC, where a 1 Sv ( $1 \text{ Sv} = 10^6 \text{ m}^3/\text{sec}$ ) increase in the AMOC would yield a  
290  $0.05 \pm 0.01$  PW increase in the meridional heat transport. Barreiro et al. (2008), analyzed  
291 the products of two models (ECBILT-CLIO and GFDL-CM2.1), and obtained a  
292 correlation of 0.7 between the heat transport across 30°S and the AMOC intensity in the  
293 basin.

294

295 Changes in the heat transport across 30°S are also noticed in the circulation of the eastern  
296 boundary. Numerical experiments show that a freshening in the North Atlantic induces a  
297 surface warming in the Benguela upwelling region (e.g. Stouffer et al., 2006). This can be  
298 understood as a consequence of the deepening of the local thermocline due to a decreased  
299 equator-to-subtropics surface density gradient that affects the surface wind-driven  
300 circulation (Fedorov et al., 2007; Barreiro et al., 2008). These modeling results indicate  
301 that the coastal upwelling region in the southeastern Atlantic may be another key region  
302 for future indirect monitoring of the changes in the Atlantic Ocean heat transport.

303

#### 304 **4. The South Atlantic water mass transformations**

305 The South Atlantic contains two of the most energetic regions of the world ocean: the  
306 confluence of the Malvinas and Brazil Currents on the western side of the basin, and the  
307 retroflection of the Agulhas Current in the eastern side (Legeckis and Gordon, 1982;  
308 Garnier et al., 2003). The encounter of the warm and saltier southward flowing Brazil  
309 Current with the cold and fresh northward flowing Malvinas Current (a branch of the  
310 Antarctic Circumpolar Current was first denominated the Confluence by Gordon (1986).  
311 The location of the Confluence varies in time and space due to the internal dynamics of  
312 the system and the seasonal variations of the wind stress forcing (Olson et al., 1988;  
313 Gordon and Greengrove, 1986; Garzoli, 1993; Matano et al., 1993). In addition to the  
314 annual cycle, anomalous northward penetrations of the Malvinas Current have been  
315 attributed to changes in the winds at the Drake Passage (Garzoli and Giullivi, 1994).  
316 South of Africa, the Agulhas Current enters the Atlantic, retroflects and, in the process

317 shed large energetic rings that carry Indian Ocean waters into the Atlantic (e.g.,  
318 Duncombe Rae et al., 1996; Goni et al., 1997; Speich et al., 2002; Lutjeharms et al, 1996;  
319 Garzoli et al., 1999). The large variability in these boundary regions not only reflects  
320 internal ocean dynamics but also energetic interocean exchanges with the South Pacific  
321 and South Indian oceans. Also to be considered is that the Antarctic Circumpolar Current,  
322 one of the stronger currents of the globe, constitutes the South Atlantic southern  
323 boundary. It is therefore to be expected that the South Atlantic acts as a strong source of  
324 mixing and water mass transformation for the compensating flows.

325

326 The complexity of the South Atlantic's water mass structure reflects its connections to  
327 the neighboring basins. The SACW (South Atlantic Central Waters) found in the  
328 subtropical gyre are produced locally (e.g. Stramma and England, 1999). The AAIW has  
329 two sources: it originates from a surface region at the Brazil Malvinas Confluence north  
330 of the Drake Passage, and it also receives an injection of water from the Indian Ocean as  
331 part of the Agulhas/Benguela current system. The sources of the Benguela Current  
332 (Garzoli and Gordon, 1996) include Indian and South Atlantic subtropical thermocline  
333 water; saline, low-oxygen tropical Atlantic water; and cooler, fresher subantarctic water.  
334 In the area between the continental shelf and Walvis Ridge it was found that 50% of the  
335 source water came from the central Atlantic, 25% came from the Indian Ocean, and 25%  
336 came from the Agulhas Current and the tropical Atlantic (Garzoli and Gordon, 1996).  
337 Schmid and Garzoli (2010) analyzed hydrographic and trajectory data collected with  
338 Argo floats. The analysis show interesting new results on the spreading of the AAIW in  
339 the Atlantic, among others, show indications for a southward spreading of AAIW from



340 the equator to the eastern boundary.

341 A complex vertical structure of water masses is also observed in the southwestern  
342 Atlantic due to the poleward penetration of subtropical waters associated with the Brazil  
343 Current and the equatorward penetration of subantarctic waters associated with the  
344 Malvinas Current. These various water masses contribute even more to this very complex  
345 dynamical confluence zone. At the surface, the Brazil Current carries subtropical water  
346 and the Malvinas Current subantarctic Surface Water. After the two currents collide,  
347 although there is some mixing, the most robust structure is the thermohaline front that  
348 separates the water masses. Below the first 1000 km, there is AAIW flowing equatorward  
349 and there is also evidence of westward flowing Weddell Sea deep water at the very  
350 bottom of the Brazil-Malvinas Confluence Zone (Cunningham and Barker, 1996).  
351 Between the AAIW and the Weddell Sea deep water there are three different water masses  
352 flowing poleward: North Atlantic Deep Water, Lower Circumpolar Deep Water, and  
353 Upper Circumpolar Deep Water (Piola and Gordon, 1989; Talley, 2003; Stramma and  
354 England, 1999; Sloyan and Rintoul, 2001).

355

356 As an example of the different water masses in the South Atlantic, the trajectory of an  
357 Argo float deployed in the South Pacific west of the Drake Passage cruising the Atlantic  
358 towards the Indian Ocean is shown in Figure 4. The float, parked at a nominal depth of  
359 1000m, surface every 10 days collecting hydrographic data during its mission that is  
360 transmitted to the Argo data centers in real time. The float was deployed in October 2005  
361 and by April 2010 it is approaching the Indian Ocean. The hydrographic data collected by  
362 float shows the changes of the water mass distributions along the way. The profiles are

363 color coded to show these transitions. The float followed the Antarctic Circumpolar  
364 Current, loops into the Malvinas Current and flows east from the confluence region  
365 (Figure 4 a). The time depth distribution of the salinity field is shown in Figure 4b, and  
366 the vertical profiles in Figure 4 c. The T/S diagrams (Figure d) show the transition  
367 between the water masses as the float moves towards the east. The subantarctic mode  
368 water (in blue) sinks at the confluence to forms the AAIW. The isopycnal 27.0 and 27.5  
369 mark the transition between the SACW and the AAIW.

370

371 In a comprehensive inverse study of water mass transformations, Sloyan and Rintoul  
372 (2001) combined hydrographic data collected south of 12°S. They concluded that within  
373 the Atlantic sector of the Southern Ocean there is a transformation of Antarctic surface  
374 water into lower South Atlantic Mode Water (SAMW). This conversion occurs in the  
375 southwestern Atlantic near the Confluence region and it is attributed to air-sea  
376 interaction. Another significant water mass transformation (about 6 Sv) occurs further  
377 north between the Argentine basin and the mid Atlantic ridge at approximately 20°W.  
378 Here thermocline water is transformed to upper SAMW by air-sea interaction. At the  
379 eastern side of the basin, the South Atlantic Current meets with the westward injection of  
380 Indian Ocean waters carried by the Agulhas Current leading to water mass exchanges  
381 through the Agulhas leakage and in the retroflexion and the rings shed during the  
382 process. These mesoscale interactions have an impact on the MOC through the  
383 transformation and subduction of SAMW and AAIW (Hazeleger and Drijhout, 2000;  
384 Schmid et al., 2003)

385

386 Several attempts have been made during the last few years to estimate the South  
387 Atlantic's water mass transformations using state-of-the-art eddy-permitting numerical  
388 simulations. Donners et al. (2005) observed that in the South Atlantic portion of OCCAM  
389 (Ocean Circulation and Climate Advanced Modeling, Webb et al., 1997), intermediate  
390 waters are imported from the Pacific and light surface waters are imported from the  
391 Indian Ocean. In return SACW and denser water masses are exported to the Indian  
392 Ocean. It was observed that while surface water abducts in the South Atlantic, all  
393 other water masses experience a net subduction. The subducted AAIW and SAMW  
394 reemerge mainly in the Antarctic Circumpolar Current farther downstream while lighter  
395 waters reemerge in the eastern tropical Atlantic. Thus most of the northward export of  
396 South Atlantic waters is constrained to the surface waters.

397

398 Schouten and Matano (2003) investigated the formation of mode waters and intermediate  
399 waters in the Southern Ocean from POCM. The model reproduces the MOC in the world  
400 ocean. The zonally integrated Meridional Overturning stream function in neutral  
401 coordinates for the Atlantic south of 20°S is shown in Figure 5 (left panel). The dashed  
402 lines indicate what part of the overturning occurs within the mixed layer. In the Southern  
403 Ocean, most of the overturning is confined to the mixed layer and associated with  
404 seasonal variability. In the same study, Schouten and Matano (2003) calculated the model  
405 transports in isopycnal layers across 30°S. The transports can be interpreted as diapycnal  
406 transformations within the basins. In the Atlantic (Figure 5 right panel), a meridional  
407 overturning circulation of 17 Sv is observed. Results show that eddy fluxes of heat and  
408 buoyancy play an important role in the formation of the intermediate waters by

409 transferring water from the southern parts of the subtropical gyres into the ACC and vice  
410 versa. The effects of eddy fluxes are strongly concentrated in the Cape Basin and the  
411 Brazil-Malvinas Confluence in the Atlantic Ocean.

412

413 Although the analysis of Schouten and Matano (2003) highlighted the contribution of the  
414 South Atlantic circulation to the overall water mass balance, its focus was not the South  
415 Atlantic but the Southern Ocean. To advance these matters we evaluated the water mass  
416 transformation within the South Atlantic basin using the results of the same model. The  
417 volume transports in neutral density layers are computed and the mean convergence or  
418 divergence within a given density range is equivalent to the removal or formation of  
419 water due to diapycnal processes. Density changes in the upper 1000 m are below 0.1  
420 kg/m<sup>3</sup> for most of the southern hemisphere. As diapycnal transformations are found to  
421 modify water masses at far higher rates, possible model drifts are neglected and steady  
422 state is assumed. The isopycnal transports in 4°x 4° boxes between 70°S and 20°N are  
423 then computed. The convergence or divergence of the transport in a given isopycnal layer  
424 can be interpreted as diapycnal removal or formation. Volume divergences in 4°x4°  
425 horizontal boxes and in discrete sigma levels were first computed. These boxes were then  
426 grouped in seven distinct regions (Fig. 6, upper panel). Results are shown in Figure 6,  
427 lower panel. The model results shows significant water mass conversions within the  
428 South Atlantic, particularly in regions of intense mesoscale variability such as the  
429 southwestern Atlantic and the Cape Basin. The signs and magnitude of the conversions  
430 indicated by the model are in good agreement with those suggested by the observations,  
431 showing a conversion from surface and deep waters into intermediate waters in the

432 southwestern Atlantic and from intermediate into surface waters in the Cape Basin region  
433 (Sloyan and Rintoul, 2001; Piola et al., 2000). Near the tropics there is a net conversion  
434 of intermediate into surface waters. As it was shown in the previous section, a heat  
435 balance of POCM reveals that the passage of these water masses at 30°S generates a  
436 northward heat flux of 0.55 PW, a value very close to the 0.50 PW recently estimated  
437 from observations by Garzoli and Baringer (2007). The model balances are also  
438 consistent with the canonical circulation schemes derived from observations (e.g.,  
439 Gordon et al., 1992) and they highlight two important characteristics of the South  
440 Atlantic circulation, namely that there is an active water mass transformation within the  
441 South Atlantic basin, and that a large portion of this transformation occurs in the highly  
442 energetic boundary regions.

443

444 The previous results indicate that the Brazil/Malvinas Confluence and the Cape Basin  
445 region are not only the main gateways for the entrainment of thermocline waters from  
446 neighboring oceans, but also for their modification. Considering the high levels of  
447 variability of these regions it is expected that the intense mixing associated with this  
448 variability will affect the regional water mass structure. Little is known about the  
449 dynamical mechanisms that control the variability of these intensely energetic boundary  
450 regions. For example, it is unknown whether or not the Confluence variability is  
451 influenced by the ACC variability, or if the shedding of Agulhas rings is modulated by  
452 the low frequency variability of the South Indian Ocean. Such topics are not only relevant  
453 to our understanding of the local dynamics, but also to the mechanisms that regulate the  
454 inflow and outflows through these choke points of the global thermohaline circulation. In

455 what follows we will expand the discussion on the questions posed by the models on  
456 these two regions in particular, and for the open basin in general.

457

## 458 **5. South Atlantic interocean exchanges**

459 The South Atlantic interocean exchanges are a weighty element of the MOC; without  
460 them, the dense waters produced in the North Atlantic would not be able to spread to the  
461 Indian and Pacific basins and the lighter waters produced therein would not be able to  
462 reach the North Atlantic. The South Atlantic not only facilitates the interocean  
463 exchanges, but it may also set preferential paths of communication. Although the strength  
464 of the MOC is determined by convection in the North Atlantic, this convection is highly  
465 sensitive to the properties of the returning flow, specifically to whether it is dominated by  
466 contributions from the Indian or the Pacific Oceans. Thus, convection in the North  
467 Atlantic is, to a large extent, dependent on what type of water mass the South Atlantic  
468 exports. If the inflows from the Indian and Pacific Oceans had similar water mass  
469 characteristics, then the mechanisms controlling the South Atlantic circulation (and its  
470 interocean exchanges) would be largely irrelevant to the MOC variability. The crux of the  
471 problem, however, is that the Indian and the Pacific water masses have marked  
472 differences. Changes in the ratio of entrainment from these distinct sources have  
473 profound implications for the stability and variability of the MOC (e.g. Weijer et al.,  
474 2001; Biastoch et al., 2009). Paleooceanographic data indicates that the transition from the  
475 last glacial conditions, and the resumption of the MOC, were correlated with a  
476 strengthening of the inflow from the Indian Ocean suggesting a crucial role of the  
477 Agulhas leakage in glacial terminations and the resulting resumption of the AMOC

478 (Peeters et al., 2004). Since most of the South Atlantic interocean exchange is mediated  
479 by highly energetic western boundary currents, the question of what controls the  
480 variability of the interocean exchanges can therefore be rephrased in terms of what  
481 controls the variability of its western boundary currents. In particular, for the major  
482 western boundary currents the Malvinas Current, which connects the South Atlantic to  
483 the Pacific Ocean, and the Agulhas leakage, which connects the South Atlantic to the  
484 Indian Ocean.

485

486 The contribution of the Malvinas Current to the MOC is twofold, first it injects the  
487 relatively fresh and cold intermediate waters into the South Atlantic that are ultimately  
488 drawn into the North Atlantic and, second, it contributes to the observed water mass  
489 transformations in the Argentinean Basin (see Section 4). The links between the  
490 variability of the Malvinas Current and the atmospheric and oceanic circulation in the  
491 Southern Ocean are not well established, but all evidence suggests that low-frequency  
492 variations in the Malvinas Current transport are connected to variations of the Antarctic  
493 Circumpolar Current transport in the Drake Passage, wind stress forcing in the  
494 circumpolar region, and the propagation of eddies from the South Pacific Basin (Garzoli  
495 and Giulivi, 1989; Vivier and Provost, 2001; Fu, 2006; Fetter and Matano, 2008;  
496 Spadone and Provost, 2009) . Analysis of the POCM model (Fetter and Matano, 2008)  
497 showed that the observed low correlation between the transport variations of the  
498 Antarctic Circumpolar Current and the Malvinas Current is masked by higher frequency  
499 variability. They also showed that as part of this high variability there are anomalies that  
500 propagate to the interior and that affect the transports at the boundaries of the South

501 Atlantic.

502

503 Following Fetter and Matano, (2008), the POCM product was analyzed together with  
504 wind stress products and sea surface height anomalies from AVISO altimetry  
505 (<http://www.aviso.oceanobs.com/>). A Principal Estimator Patterns (PEP) analysis (e.g.,  
506 Davis, 1977; Fetter and Matano, 2008) was conducted between SSH anomalies and the  
507 wind stress curl. Results of the analysis are shown in Figure 7. The top panel shows the  
508 amplitude of the SSH anomaly as derived from the Aviso product, and the middle panel  
509 those of the wind curl as derived from the European Centre for Medium-Range Weather  
510 Forecasts (ECMWF) winds. The lower panel shows the time series of the first PEP  
511 estimator of model product and the AVISO data. There is a strong coherence between  
512 the two series, reinforcing the validity of the model to perform the analysis. Interesting to  
513 note is that the maximum amplitude in SSH observed at the Brazil Malvinas Confluence,  
514 approximately centered at 300° W and 40°S (Figure 7, top panel) is out of phase with a  
515 maximum of the curl of the wind stress in the South Pacific centered at around 250°W  
516 and is in phase with the anomalies south of Australia at 80°W. This is an indicator of a  
517 strong correlation of the variability of the winds in the Southern Ocean and the variability  
518 of the western boundary currents in the South Atlantic. There is not enough evidence to  
519 assess the impact of the Malvinas Current variability on the MOC. However, as it was  
520 shown in the previous section, model results and observations indicate that it contributes  
521 to water mass transformation in the Argentinean Basin (e.g., Fig. 5). Only a relatively  
522 small portion of the Malvinas Current waters are entrained in the subtropical gyre and  
523 funneled to the North Atlantic. This mostly occurs in the Agulhas Retroflexion region



524 where a portion of the South Atlantic Current diverts north to feed the Benguela Current.  
525  
526 Due to its direct connection to the subtropical gyre there are more studies on the Agulhas  
527 Current impact on the MOC. Donners and Drijfhout (2004) estimated that 90% of the  
528 upper branch of the AMOC is derived from the inflow of Indian Ocean water into the  
529 South Atlantic. Biastoch et al. (2008) argued that the Agulhas leakage is a source of  
530 decadal MOC variability. According to this hypothesis, low frequency signals induced  
531 by the Agulhas are carried across the South Atlantic by Rossby waves and into the North  
532 Atlantic along the American continental slope. The resulting signal in the AMOC  
533 transport gradually diminishes from south to north, but has an amplitude in the tropical  
534 Atlantic of comparable magnitude to the effect of subarctic deep water. (Biastoch et al,  
535 2009) also show that the transport of Indian Ocean waters into the South Atlantic via the  
536 Agulhas leakage has increased during the past decades in response to the change in wind  
537 forcing. Studies based on paleo data and simplified models (Weijer et al., 1999; Peeters et  
538 al., 2004) concluded that a shutdown of the Agulhas Current influences the deep water  
539 formation in the North Atlantic with obvious consequences for the MOC. In a recent  
540 publication, Haarsma et al. (2009) used a coupled ocean-atmosphere model to investigate  
541 the impact of the Agulhas leakage on the Atlantic circulation. The experiments performed  
542 mimic the closure of the warm water path in favor of the cold water path. Their results  
543 reinforce the role of the Agulhas leakage on the AMOC; the modified water  
544 characteristics due to the shut down of the Agulhas leakage remain unaffected when  
545 crossing the equatorial region and therefore are capable of affecting the deep water  
546 formation in the North Atlantic.

547

548 Goni et al. (1997) observed that there is a close correlation between the transport of the  
549 Agulhas Current and the shedding of rings. Altimeter data analysis indicates that the  
550 Agulhas rings are modulated by the flow through the Madagascar Current and the  
551 Mozambique Channel. Analysis of altimeter data showed significant interannual  
552 variations in the rate of Agulhas ring shedding (Goni et al., 1996; Quartly and Srokosz,  
553 2002). These studies lead to the conclusion that low-frequency (interannual and longer)  
554 variations in the interocean exchange around South Africa are linked to large-scale modes  
555 of climate variability.

556

557 Although there are far more studies on the impact of the Agulhas Current on the MOC,  
558 observations indicate that at least half of the northward upper ocean flux transported by  
559 the Benguela Current is from subpolar origin, i.e., it is ultimately derived from the  
560 Malvinas Current. In fact, Garzoli et al. (1997) noted that although the annual mean  
561 value of the Benguela Current transport ( $\sim 13$  Sv), changes less than 20% from year to  
562 year, there are marked interannual transitions in the sources from which it drains its  
563 waters, i.e., the South Atlantic Current or the Agulhas Current. This observation raises  
564 the question of whether years of strong South Atlantic inflow can be characterized as cold  
565 path years while those of strong Agulhas inflow can be characterized as warm path years.  
566 The nature of the mechanisms that would regulate the dominance of one path over the  
567 other is unknown. Whether changes in the sources of the Benguela transport can really  
568 affect the inter-hemispheric exchange is another unknown question.

569

570 **6. Summary and discussion:**

571 Observations and models consistently indicate that the South Atlantic is not just a passive  
572 conduit for the passage of water masses formed in other regions of the world ocean but  
573 instead actively participates in their transformation. They occur across the entire basin,  
574 but are intensified in regions of high meso-scale variability, particularly at the  
575 Brazil/Malvinas Confluence and the Agulhas Retroflexion region. It has also been  
576 argued that the South Atlantic circulation may set preferential paths for interocean  
577 exchanges. Observations show interannual variations in the sources that feed the  
578 Benguela Current and hence in the northward cross-equatorial fluxes. It has also been  
579 shown that processes occurring in the Southern Ocean and the adjacent basins alter this  
580 variability. There are dynamical processes that link the South Atlantic to the other basins  
581 and that mediate the observed water mass transformations. In spite of this mounting  
582 evidence on the contribution of the South Atlantic to the MOC it is obvious that still there  
583 are more questions about this portion of the MOC than answers. To advance our  
584 understanding of the MOC and its climatic implications it is imperative to expand the  
585 existing observing systems towards other important regions, particularly those like the  
586 South Atlantic containing strategic choke points of the MOC. This will allow us not only  
587 to document climatically important phenomena, but also to improve our capacity to  
588 forecast them. Ongoing and new observations should have three major foci: (1) regions  
589 where topography significantly alters the deep circulation; (2) choke points where deep  
590 water is exchanged between the major ocean basins (e.g. Drake Passage); and (3) deep  
591 strong flows where the major water masses are carried significant distances within basins.  
592 A South Atlantic monitoring system should measure the meridional heat transport and its

593 variability along a zonal line across the basin. Observations at the boundaries should  
594 provide information on the DWBC passages and intensity. The upper limb of the MOC,  
595 carrying AAIW at mid latitudes, the role of the Agulhas rings, and leakage in these  
596 transfers should be further investigated. To advance our understanding of the MOC  
597 pathways it is necessary to determine the influence of the bottom topography on the mean  
598 circulation. For example, it is necessary to establish how the mid-Atlantic Ridge affects  
599 the water mass transformation and meridional fluxes. What happens at the bifurcation of  
600 the South Equatorial Current where the DWBC breaks into eddies? How is it  
601 reconstituted again at mid latitudes as observations show both at the eastern and western  
602 boundaries? Different deep-water masses separated by topographic features can mix and  
603 exchange properties. The highest priority sites in the Atlantic are the Weddell Sea, the  
604 Vema Channel and the Romanche Fracture Zone sill in the South Atlantic, and in the  
605 Samoan Passage, Denmark Straits, and Cape Farewell in the North Atlantic.

606

607 Our capacity to establish efficient monitoring systems can be greatly improved by  
608 dedicated modeling studies of the South Atlantic circulation and its connection to the  
609 neighboring basins. High-resolution models could help to determine the optimal location  
610 and minimum requirements for a monitoring system designed to measure components of  
611 the MOC in the South Atlantic Ocean. The failure of some state-of-the-art global eddy-  
612 resolving models to resolve critical aspects of the MOC such as the path of the Agulhas  
613 rings highlights our need to focus our attention on this climate-relevant region. If, as  
614 observed, a numerical model fails to reproduce the correct path of the Agulhas eddies it  
615 will produce the wrong meridional heat and salt fluxes, and hence will distort the

616 structure of the MOC. As we strive to move from coarse-resolution to high-resolution  
617 climate models these issues need the pressing attention of the modeling community.  
618 Equally alarming is the observed failure of these models to reproduce the formation of  
619 the Zapiola Anticyclone in the Argentinean Basin. The evidence presented herein  
620 indicates that this is an active region for water mass formation. Models that fail to  
621 reproduce this particular feature, however, are likely to grossly underestimate this  
622 important component of the South Atlantic circulation.

623

624 The limitations of this paper, that poses more scientific questions than answers, points  
625 towards the need for sustain observations in the South Atlantic and Southern Oceans in  
626 conjunction with modeling efforts that will help to increase our understanding of the most  
627 important processes and allow us to formulate meaningful climate predictions.

628

629

629 **References**

630

631 Baringer, M.O., and Garzoli, S.L., 2007. Meridional heat transport determined with  
632 expendable bathythermographs, Part I: Error estimates from model and  
633 hydrographic data. *Deep-Sea Res., I*, 54(8):1390-1401.

634 Baringer, M.O., and Larsen, J.C., 2001. Sixteen years of Florida Current transport at  
635 27°N. *Geophys. Res. Lett.*, 28(16):3179-3182.

636 Barreiro, M., Fedorov, A., Pacanowski, R., Philander, G., 2008. Abrupt climate changes:  
637 How freshening of the northern Atlantic affects the thermohaline and wind-driven  
638 oceanic circulations. *Rev. Earth. Planet Sci.* Copyright © 1996 Published by  
639 Elsevier Science Ltd.

640 Biastoch, A., Böning, C.W., Schwarzkopf, F.U., Lutjeharms, J.R.E., 2009. Increase in  
641 Agulhas leakage due to poleward shift of Southern Hemisphere westerlies. *Nature*,  
642 462, doi:10.1038/nature08519.

643 Boebel, O., Lutjeharms, J., Schmid, C., Zenk, W., Rossby, T., Barron, C., 2003. The  
644 Cape Cauldron: a regime of turbulent inter-ocean exchange. *Deep-Sea Res.*, 50, 57-  
645 86(30).

646 Broecker, W.S., and Peng, T-H., 1982. *Tracers in the Sea*. 690 pp, Lamont Doherty  
647 Geological Observatory, Palisades, NY. (Eldigio, Palisades, 1982).

648 Broecker, W.S., 1991. The great Conveyor Belt, *Oceanogr.*, 4 (2), 79-89.

649 Bryden, H. L., Longworth, H. R., and Cunningham, S. A., 2005. Slowing of the Atlantic  
650 Meridional Overturning Circulation at 26.5°N., *Nature*, 438, 655-657.

651 Campos, E.J.D., Lorenzetti, J., Stevenson, M., Stech, J.L., and de Souza, R.B., 1996.

652 Penetration of Waters from the Brazil-Malvinas Confluence Region Along the  
653 South American Continental Shelf up to 23°S. *An. Acad. Bras. Ci.*, 68, No.  
654 1/Suppl., pp. 49-58.

655 Cunningham, S.A., Kanzow, T., Rayner, D., Baringer, M.O., Johns, W.E., Marotzke, J.,  
656 Longworth, H.R., Grant, E.M., Hirschi, J.J.-M., Beal, L.M., Meinen, C.S., Bryden,  
657 H.L., 2007. Temporal Variability of the Atlantic Meridional Overturning  
658 Circulation at 26.5°N. *Science*, 317. 5840, 935 – 938, DOI 10.1126/science.  
659 1141304.

660 Cunningham, A.P. and Barker, P.F., 1996. Evidence for westward-flowing Weddell Sea  
661 Deep Water in the Falkland Trough, western South Atlantic. *Deep-Sea Res.*, 43,  
662 643-654.

663 de las Heras, M.M., Schlitzer, R., 1999. On the importance of intermediate water flows  
664 for the global ocean overturning. *J. Geophys. Res.* 104, 15515–15536.

665 Davis, R. E., 1977. Techniques for statistical analysis and prediction of geophysical fluid  
666 systems, *Geophys. Astrophys. Fluid Dyn.*, 8, 245 – 277,  
667 doi:10.1080/03091927708240383.

668 De Ruijter, W.P.M., Biastoch, A., Drijfhout, S.S., Lutjeharms, J.R.E., Matano, R.P.,  
669 Pichevin, T., Van Leeuwen, P.J., and Weijer, W., 1999. Indian-Atlantic interocean  
670 exchange: Dynamics, estimation and impact. *J. Geophys. Res.*, 104, 20885-20910.

671 Dong, S., Garzoli, S.L., Baringer, M.O., Meinen, C.S., and Goni, G.J., 2009. Interannual  
672 variations in the Atlantic Meridional Overturning Circulation and its relationship  
673 with the net northward heat transport in the South Atlantic. *Geophys. Res. Lett.*,  
674 36(20), L20606, doi:10.1029/2009GL039356.

675 Donners, J., and Drijfhout, S.S., 2004. The Lagrangian View of South Atlantic Interocean  
676 Exchange in a Global Ocean Model Compared with Inverse Model Results. *J. Phys.*  
677 *Oceanogr.* 34, 1019–1035.

678 Donners, J., Drijfhout, S.S., and Hazeleger, W., 2005. Water Mass Transformation and  
679 Subduction in the South Atlantic. *J. Phys. Oceanogr.*, 35, 10, 1841-1860.

680 Duncombe Rae, C.M., Garzoli, S.L., and Gordon, A.L., 1996. The eddy field of the  
681 southeast Atlantic Ocean: A statistical census from the Benguela Sources and  
682 Transports (BEST) project. *J. Geophys. Res.*, 101(C5), 11, 949- 11,964

683 England, M.H., Garcon, V.C., and Minster, J.-F., 1994. Chlorofluorocarbon uptake in a  
684 World Ocean model, 1. Sensitivity to the surface gas forcing. *J. Geophys. Res.*, 99,  
685 25215-25233.

686 Fedorov, A., Barreiro, M., Boccaletti, G., Pacanowski, R., Philander, G., 2007. The  
687 freshening of surface waters in high latitudes: Effects on the thermohaline and  
688 wind-driven circulations. *J. Phys. Oceanogr.*, 37, 896-907.

689 Fetter, A. F. H and Matano, R., 2008. On the Origins of the Variability of the Malvinas  
690 Current in a Global, Eddy-Permitting Numerical Simulation. *J. Geophys. Res.*, 113,  
691 C11018, doi: 10.1029/2008JC004875.

692 Fu, L.L., 1981. The general circulation and meridional heat transport of the subtropical  
693 South Atlantic determined by inverse methods. *J. Phys. Oceanogr.* 11, 1171–1193.

694 Fine, R. A., 1985. Direct evidence using tritium data for throughflow from the Pacific  
695 into the Indian Ocean. *Nature*, 315, 478-480.

696 Ganachaud, A.S., and Wunsch, C., 2003. Large-scale ocean heat and freshwater  
697 transports during the World Ocean Circulation Experiment. *J. Climate*, 16, 696–



698           705.

699   Garzoli, S.L., 1993. Geostrophic velocity and transport variability in the Brazil-Malvinas  
700           Confluence. *Deep-Sea Res.*, 40(7):1379-1403

701   Garzoli, S.L., Goni, G.J., Mariano, A., and Olson, D., 1997. Monitoring South Eastern  
702           Atlantic Transports using altimeter data. *Jour. Mar. Res.*, 55, 453-481.

703   Garzoli, S.L. and Baringer, M.O., 2007. Meridional Heat Transport determined with  
704           Expendable Bathythermographs. Part II: South Atlantic Transport. *Deep-Sea Res. I*,  
705           54 1402–1420.

706   Garzoli, S.L., Giulivi, C., 1994. What forces the variability of the southwestern Atlantic  
707           boundary currents? *Deep-Sea Res. I*, 41, 1527–1550.

708   Garzoli, S.L., Gordon, A.L., 1996. Origins and variability of the Benguela Current. *J.*  
709           *Geophys. Res.*, 101, 897–906.

710   Garzoli, S.L., Richardson, P.L., Dumcombe Rae, C.M., Fratantoni, D.M., Goni, G.J., and  
711           Roubicek, A.J., 1999. Three Agulhas rings observed during the Benguela Current  
712           Experiment. *J. Geophys. Res.*, 104(C9): 20,971-20,986.

713   Ganachaud, A.S., and Wunsch, C., 2003. Large-scale ocean heat and freshwater  
714           transports during the World Ocean Circulation Experiment. *J. Climate.*, 16, 696–  
715           705.

716   Goni, G.J., Garzoli, S.L., Roubicek, A.J., Olson, D.B., and Brown, O.B., 1997. Agulhas  
717           ring dynamics from TOPEX/POSEIDON satellite altimeter data. *J. Mar. Res.*,  
718           55(5):861-883.

719   Goni, G. J., Bringas, F., and DiNezio, P., 2010. Low frequency variability of the Brazil  
720           Current Front. *Deep-Sea Res.*, submitted.

721 Gordon, A., 1985. Indian-Atlantic Transfer of Thermocline Water at the Agulhas  
722 Retroflection. *Science*, 227, 4690, 1030 – 1033, DOI:  
723 10.1126/science.227.4690.1030

724 Gordon, A.L., Greengrove, C.L., 1986. Geostrophic circulation of the Brazil–Falkland  
725 confluence. *Deep-Sea Res.*, 33, 573–585.

726 Gordon, A. L., 1986. Interocean exchange of thermocline water, *J. Geophys. Res.*, 91,  
727 5037-5046.

728 Gordon, A. L. and Piola, A., 1983. Atlantic Ocean upper layer salinity budget. *Phys.*  
729 *Oceanogr.*, 13, 1293-1300.

730 Gordon, A. L., 1989. Brazil-Malvinas confluence in 1984. *Deep-Sea Res.*, 36, 359-384.

731 Gordon, A.L., Weiss, R.F., Smethie, W.M., Warner, M.J., 1992. Thermocline and  
732 Intermediate Water Communication between the South-Atlantic and Indian Oceans.  
733 *J. Geophys. Res. Oceans.*, 97, C5, 7223- 7240.

734 Haarsma, R.J., Selten, F.M., Weber, S.L., and Kliphuis, M., 2005. Sahel rainfall  
735 variability and response to greenhouse warming. *Geophys. Res. Lett.*, 32, L17702.

736 Hansen, J.E., Ruedy, R., Sato, M., Imhoff, M., Lawrence, W., Easterling, D., Peterson,  
737 T., and Karl, T., 2001. A closer look at United States and global surface  
738 temperature change. *J. Geophys. Res.*, 106, 23947-23963,  
739 doi:10.1029/2001JD000354.

740 Häkkinen, S.P., and Rhines, B., 2004. Global Warming and the Next Ice Age. *Science*,  
741 304, 555- 559.

742 Hazeleger, W. and Drijfhout, S.S., 2000. Eddy subduction in a model of the subtropical  
743 gyre. *J. Phys. Oceanogr.*, 30, 4, 677-695,

744 Holfort, J., Siedler, G., 2001. The meridional oceanic transports of heat and nutrients in  
745 the South Atlantic. *J. Phys. Oceanogr.*, 31, 5–29.

746 IPCC, 2007. *Climate Change 2007: The Physical Science Basis. Contribution of Working*  
747 *Group I to the Fourth Assessment Report of the Intergovernmental Panel on*  
748 *Climate Change*, 996 pp., Cambridge University Press, Cambridge, United  
749 Kingdom and New York, NY, USA.

750 Kanzow, T., Hirschi, J.J.-M., Meinen, C.S., Rayner, D., Cunningham, S.A., Marotzke, J.,  
751 Johns, W.E., Bryden, H.L., Beal, L.M., and Baringer, M.O., 2008. A prototype  
752 system of observing the Atlantic meridional overturning circulation: Scientific  
753 basis, measurement and risk mitigation strategies, and first results. *J. Operat.*  
754 *Oceanogr.*, 1(1), 19-28.

755 Legeckis, R., and Gordon A., 1982. Satellite Observations of the Brazil and Falkland  
756 Currents - 1975 to 1976 and 1978. *Deep-Sea Res.*, 29, 3, 375-401.

757 Lumpkin, R., and Speer, K., 2007. Global ocean meridional overturning. *J. Phys.*  
758 *Oceanog.*, 37(10):2550-2562.

759 Lumpkin, R., and Garzoli, S.L., 2010. Interannual to decadal changes in the western  
760 South Atlantic's surface circulation. *J. Phys. Oceanogr.*, submitted.

761 Lutjeharms, J.R.E. and Gordon, K., 1987. Shedding of an Agulhas Ring observed at sea.  
762 *Nature*, 325, 138-140.

763 Lutjeharms J.R.E., 1996. The exchange of water between the South Indian and South  
764 Atlantic Oceans. In: *The South Atlantic: Present and past circulation*. G. Wefer, W.  
765 H. Berger, G. Siedler, and D. Webb (eds.), 122-162, Springer-Verlag, Berlin-  
766 Heidelberg, Germany.

767 Macdonald, A. and Wunsch, C., 1996. The global ocean circulation and heat flux. *Nature*,  
768 382, 436-439.

769 Macdonald, A.M., 1996. The global ocean circulation: a hydrographic estimate and  
770 regional analysis. *Progr. Oceanog.*, 41, 281–382.

771 Macdonald, A.M., Baringer, M.O., and Ganachaud, A., 2001. Heat transport and climate.  
772 In *Encyclopedia of Ocean Sciences*, J.H. Steele, S.A. Thorpe, and K.K. Turekian  
773 (eds), London, Academic Press, 2, 1195-1206.

774 Marchisio, P., Barnier, B., and de Miranda, A.P., 1998. A sigma-coordinate primitive  
775 equation model for studying the circulation in the South Atlantic. Part II:  
776 Meridional transports and seasonal variability, *Deep-Sea Res. I*, 45, 573-608.

777 Matano, R.P., Philander, S.G.H., 1993. Heat and mass balances of the South Atlantic  
778 Ocean calculated from a numerical model. *J. Geophys. Res.* 98, 977-984.

779 Matano, R.P., Schlax, M.G., Chelton, D.B., 1993. Seasonal variability in the  
780 southwestern Atlantic. *J. Geophys. Res.*, 98, 18027–18035.

781 Matano, R.P., Beier, E.J., 2003. A kinematic analysis of the Indian/Atlantic interocean  
782 exchange. *Deep-Sea Res. II* 50, 229–249.

783 Model, F., 1950. Warmwasserheizung Europas. *Ber. Deut. Wetterdienstes*, 12, 51-60.

784 Meinen, C.S., Baringer, M.O., and Garzoli, S.L., 2006. Variability in Deep Western  
785 Boundary Current transports: Preliminary results from 26.5°N in the Atlantic.  
786 *Geophys. Res. Lett.*, 33(17):L17610, doi:10.1029/2006GL026965.

787 Nof, D. and Gorder, S.V., 1999. A different perspective on the export of water from the  
788 South Atlantic. *J. Phys. Oceanogr.*, 29, 2285-2302.

789 Østerhus, S., Turrell, W.R., Jonsson, S., and Hansen, B., 2005. Measured volume, heat,

790 and salt fluxes from the Atlantic to the Arctic Mediterranean, *Geophys. Res. Lett.*,  
791 32, L07603; doi:10.1029/2004GL022188.

792 Palastanga, V., Vera, S.C.S., and Picola, A.R., 2002. On the leading modes of sea surface  
793 temperature variability on the South Atlantic Ocean. *Exchanges*, 25.

794 Olson, D., Podesta, G., Evans, R., and Brown, O., 1988. Temporal variations in the  
795 separation of the Brazil and Malvinas Currents, *Deep-Sea Res.*, 35, 1971.

796 Peeters, F.J.C., Acheson, R., Brummer, G.-J.A., de Ruijter, W.P.M., Ganssen, G.M.,  
797 Schneider, R.R., Ufkes, E., and Kroon, D., 2004. Vigorous exchange between  
798 Indian and Atlantic Ocean at the end of the last five glacial periods. *Nature*, 430,  
799 661-665.

800 Peterson, R.G., and Stramma, L., 1991. Upper-level circulation in the South Atlantic  
801 Ocean. *Prog. Oceanogr.*, 26, 1-73.

802 Piola, A.R., and Gordon, A., 1989. Intermediate waters in the southwest South Atlantic.  
803 *Deep-Sea Res.*, 36, 1-16.

804 Piola, A.R., Campos, E.J., Möller, O.O., Charo, M., and Martinez, C., 2000. The  
805 Subtropical Shelf Front off Eastern South America. *J. Geophys. Res.*, 105, 6565 -  
806 6578.

807 Piola, A.R., and Matano, R.P., 2001. Brazil and Falklands (Malvinas) Currents., In J.H.  
808 Steele, S.A. Thorpe and K.K. Turekian (eds) *Encyclopedia of Ocean Sciences*, 1,  
809 340 - 349. London, UK: Academic Press.

810 Poole, R., and Tomczak, M., 1999. Optimum multiparameter analysis of the water mass  
811 structure in the Atlantic Ocean thermocline. *Deep-Sea Res.*, 46, 1895-1921.

812 Rintoul, S.R., 1991. South Atlantic interbasin exchange. *J. Geophys. Res.*, 96, 2675-

813           2692.

814   Rintoul, S.R., 2007. Rapid freshening of Antarctic Bottom Water formed in the Indian  
815           and Pacific Oceans. *Geophys. Res. Lett.*, 34, L06606, doi:10.1029/2006GL028550.

816   Richardson, P.L., and Garzoli, S.L., 2003. Characteristics of intermediate water flow in  
817           the Benguela Current as measured with RAFOS floats. *Deep-Sea Res. II*, 50, 87-  
818           118.

819   Saunders, P.M., King, B.A., 1995. Oceanic fluxes on the WOCE A11 section. *J. Phys.*  
820           *Oceanogr.*, 25, 1942–1958.

821   Schmid, C., Boebel, O., Zenk, W., Lutjeharms, J.R.E., Garzoli, S.L., Richardson, P.L.,  
822           and Barron, C., 2003. Early evolution of an Agulhas Ring. *Deep-Sea Res. II*, 50,  
823           141-166.

824   Schmid, C. and Garzoli, S.L., 2010. Spreading and Variability of the Antarctic  
825           Intermediate Water in the Atlantic. *J. Mar. Res.*, in press.

826   Schott, F., Dengler, M., Zantopp, R., Stramma, L., Fischer, J., and Brandt, P., 2005. The  
827           shallow and deep western boundary circulation of the South Atlantic at 5-11°S. *J.*  
828           *Phys. Oceanogr.* 35, 2031–2053.

829   Schouten, M.W., and Matano, R., 2003. Formation and pathways of intermediate water in  
830           the Parallel Ocean Circulation Model’s Southern Ocean. *J. Geophys. Res.*, 111,  
831           C06015, doi:10.1029/2004JC002.

832   Schmitz, W.J., 1995. On the interbasin-scale thermohaline circulation. *Rev. Geophys.*,  
833           33,151–173.

834   Sloyan B.M., and Rintoul, S.R., 2001. The Southern Ocean limb of the global deep  
835           overturning circulation. *J. Phys. Oceanogr.*, 31(1), 143-173.

836 Speich, S., Blanke, B., de Vries, P., Döös, K., Drijfhout, S., Ganachaud, A., and Marsh,  
837 R., 2002. Tasman Leakage: A new route for the global conveyor belt. *Geophys.*  
838 *Res. Lett.*, 29, 10, 1416, doi:10.1029/2001GL014586.

839 Srokosz M.A., 2004. New experiment deploys observing array in North Atlantic to  
840 investigate Rapid Climate Change. *Eos Trans. AGU*, 85(8), 78 & 83.

841 Sterl, A., and Hazeleger, W., 2003. Coupled variability and air-sea interaction in the  
842 South Atlantic Ocean. *Climate Dynamics*, 21, 559-571.

843 Stouffer, R.J., Yin, J., Gregory, J.M., Dixon, K.W., Spelman, M.J., Hurlin, W., Weaver,  
844 A.J., Eby, M., Flato, D.G.M., Hasumi, E.H., Hu, F.A., Jungclaus, G.J.H.,  
845 Kamenkovich, H.I.V., Levermann, I.A., Montoya, J.M., Murakami, K.S.,  
846 Nawrath, L.S., Oka, J.A., Peltier, F.W.R., Robitaille, M.D.Y., Sokolov, E.A.,  
847 Vettoretti, N.G., Webero, S.L., 2006. Investigating the Causes of the Response of  
848 the Thermohaline Circulation to Past and Future Climate Changes, *J. Climate*, 19,  
849 1365- 1387.

850 Stramma, L., and England, M., 1999. On the water masses and mean circulation of the  
851 South Atlantic Ocean. *J. Geophys. Res.*, 104, 20863–20883.

852 Speich, S., Garzoli, S.L., Piola A., 2010. A monitoring system for the South Atlantic as a  
853 component of the MOC. In *Proceedings of OceanObs09: Sustained Ocean*  
854 *Observations and Information for Society (Annex)*, Venice, Italy, 21-25 September  
855 2009, Hall, J., Harrison, D.E. & Stammer, D., Eds., ESA Publication WPP-306.

856 Talley, L.D., 1996. Antarctic intermediate water in the South Atlantic. In *the South*  
857 *Atlantic: Present and Past Circulations*. G. Wefer et al., Eds., Springer-Verlag, 219-  
858 238.

859 Talley, L.D., 2003. Shallow, intermediate, and deep overturning components of the  
860 global heat budget. *J. Phys. Oceanogr.*, 33, 530–560.

861 Toole, J., and Raymer, M., 1985. Heat and fresh water budgets of the Indian Ocean-  
862 revisited, *Deep-Sea Res.*, 32, 917-928.

863 Tokmakian, R.T., Challenor, P.G., 1999. On the joint estimation of model and satellite  
864 sea surface height anomalies. *Ocean Modelling*, 1, 39–52.

865 Tomuzak, M., and Godfrey, J.S., 1994. *Regional Oceanography: An Introduction*.  
866 Pergamon, 390.

867 Venegas, S.A., Mysak, L.A., and Straub, D.N., 1997. Atmosphere-ocean coupled  
868 variability in the South Atlantic. *J. Climate*, 10, 2904-2920.

869 Venegas, S.A., Mysak, L.A., and Straub, D.N., 1998. An interdecadal cycle in the South  
870 Atlantic and its links to other ocean basins. *J. Geophys. Res.*, 103, C11, 24, 723-24,  
871 736.

872 Webb, D.J., Coward, A.C., de Cuevas, B., and Gwilliam C.S., 1997. A multiprocessor  
873 ocean general circulation model using message passing. *J. Atmos. Oceanic*  
874 *Technol.*, 14, 175-183.

875 Weijer, W., de Ruijter, W.P.M., Sterl, A., and Drijfhout, S.S., 2002. Response of the  
876 Atlantic overturning circulation to South Atlantic sources of buoyancy. *Global and*  
877 *Planetary Change*, 34, 293-311.

878 Witter, D.L., and Gordon, A.L., 1999. Interannual variability of South Atlantic  
879 circulation from four years of TOPEX/POSEIDON satellite altimeter observations.  
880 *J. Geophys. Res.*, 104, 20, 927-20948.

881 Wüst, G., 1935. Schichtung und Zirkulation des Atlantischen Ozeans. *Die Stratosphäre*



882 des Atlantischen Ozeans, in Wissenschaftliche Ergebnisse der Deutschen  
883 Atlantischen Expedition auf dem Forschungs- und Vermessungsschiff: "Meteor"  
884 192-1927, 6, 109-228. Walter de Gruyter, Berlin.

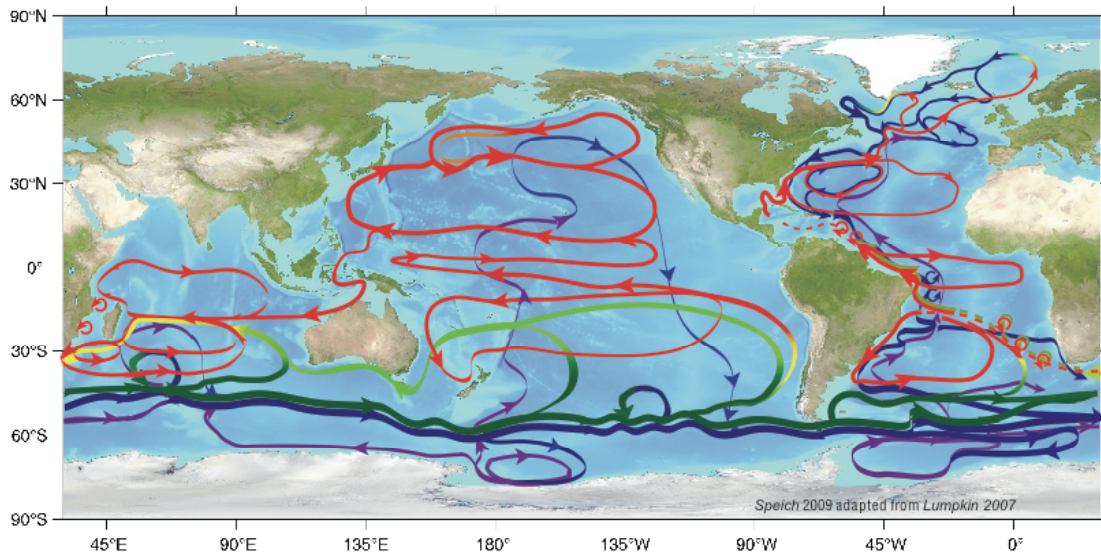
885 You, Y., 2002. Quantitative estimate of Antarctic Intermediate Water contributions from  
886 Drake Passage and the southwest Indian Ocean to the South Atlantic. J. Geophys.  
887 Res., 107, 10.1029-6.

888

889

890

890

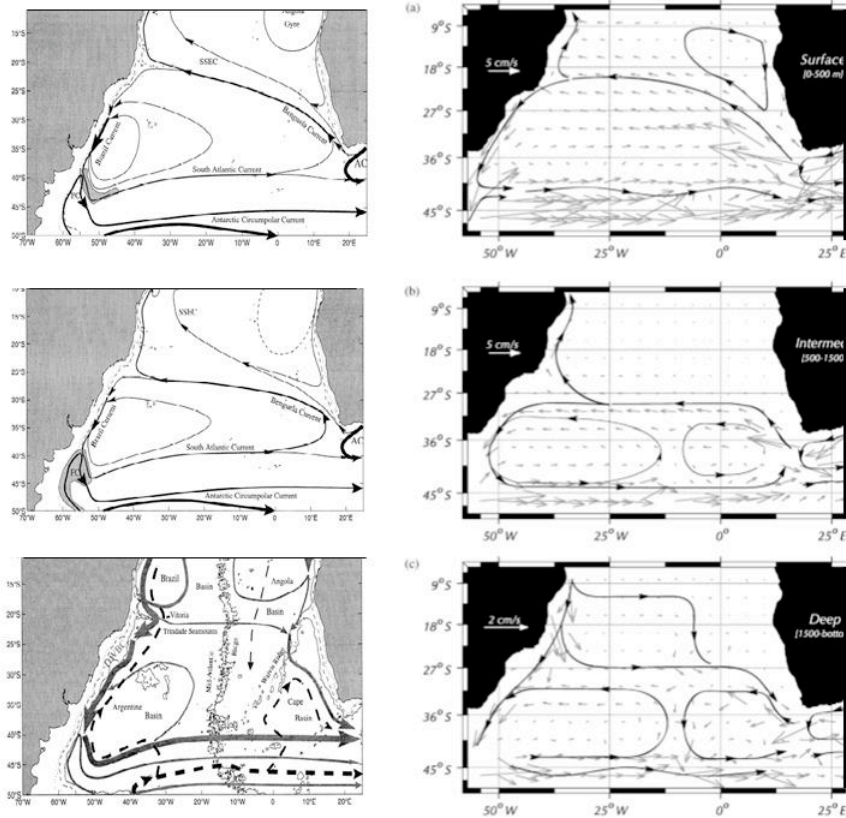


891

892

893 **Figure 1:** Schematic of the world ocean meridional overturning circulation. Red is  
894 surface flow, blue and purple are deep flows, and yellow and green represent transitions  
895 between depths (from Speich 2009, adapted from Lumpkin and Speer, 2007).

896



896

897

898 **Figure 2:** Left panel (adapted from Stramma and England, 1999) Schematic  
 899 representation of the large-scale SACW (top), AAIW (middle) and North Atlantic Deep  
 900 Water circulation (bottom). Right panel: Climatological depth-averaged velocities from  
 901 the Parallel Ocean Circulation Model (POCM-4C) at: (a) surface (0–500 m), (b)  
 902 intermediate (500–1500 m), and (c) deep (1500–bottom). The horizontal velocities were  
 903 binned in 41 x 41 boxes. The superimposed schematics show the path of the major water  
 904 masses.

905

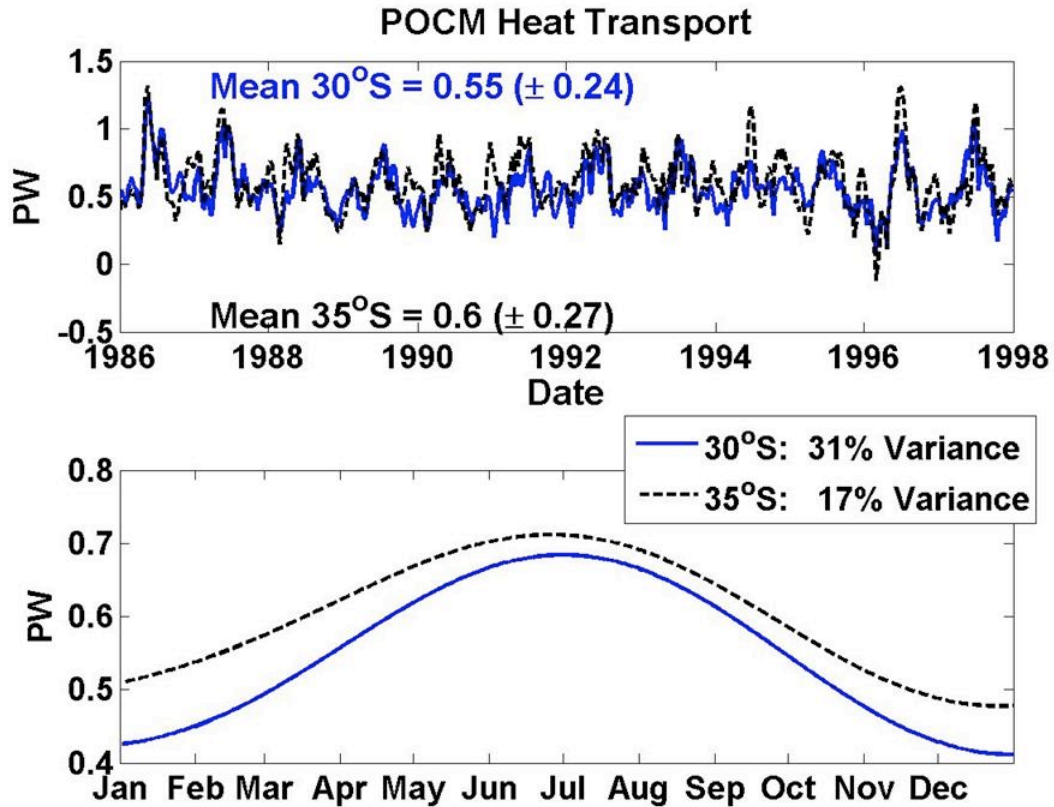
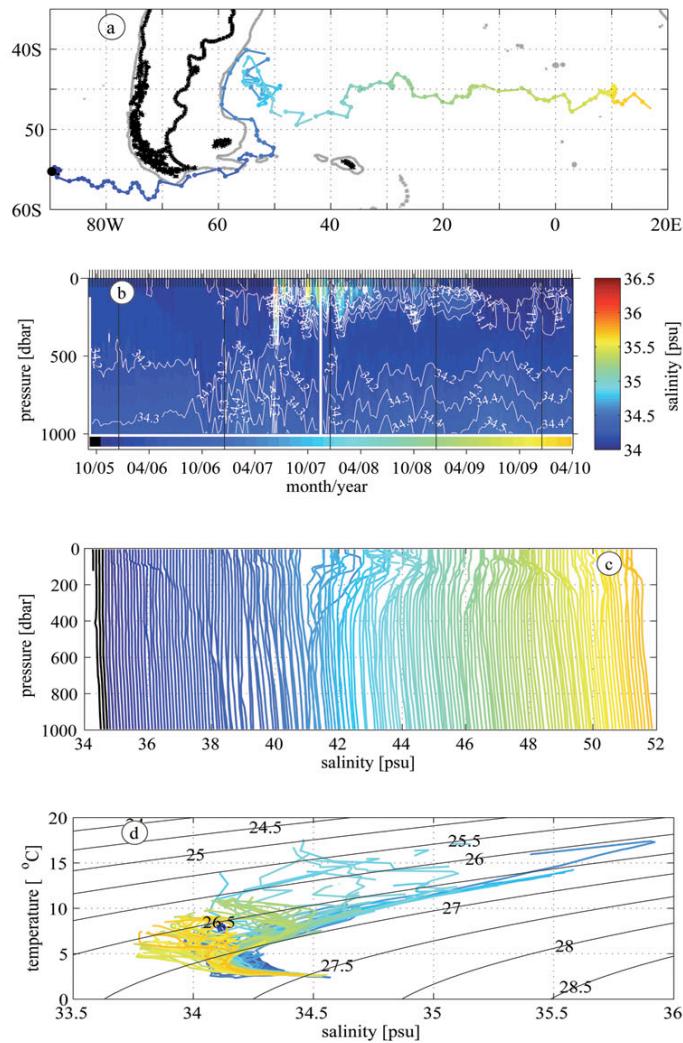


Figure 4.

905

906

907 **Figure 3:** Time series of the total heat transport (top panel) at 30°S (solid) and 35°S  
 908 (dashed) obtained from the POCM velocity and temperature fields. In parenthesis after  
 909 the mean value of the series is the standard deviation. The lower panel is the  
 910 climatological annual cycle of the heat transport (1986–1998) computed from the full-  
 911 time series at 30°S (represents 31% of the RMS variance) and at 35°S (represents 17% of  
 912 the RMS variance). (From Baringer and Garzoli, 2007).



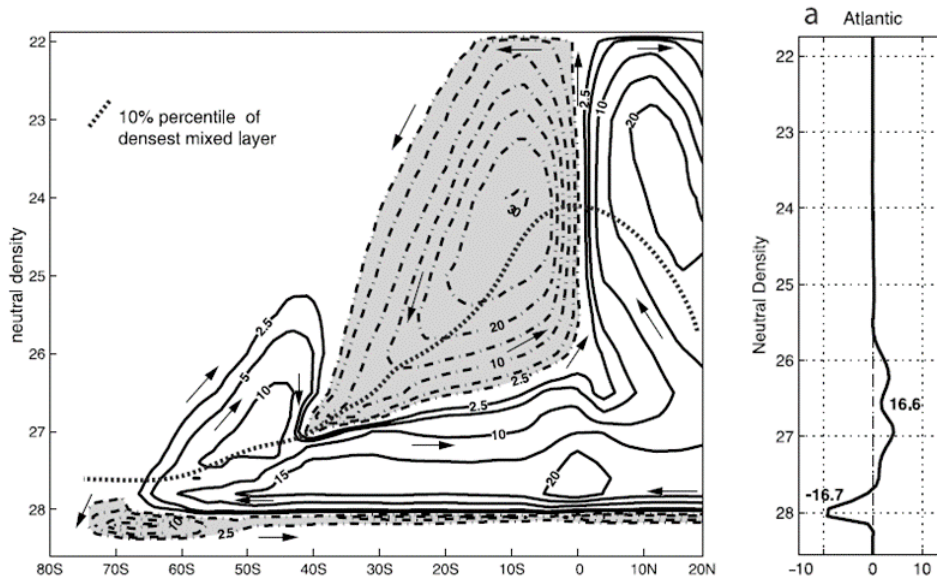
913

914

915 **Figure 4:** Trajectory of Argo float WMO 3900427 deployed in October 2005 that  
 916 transitioned from the South Pacific to the South Atlantic while drifting across different  
 917 water masses. In April 2010 the float is approaching the Indian Ocean. The top panel (a)  
 918 shows the trajectory of the float. The salinity section is shown in panel (b). Individual  
 919 vertical profiles of salinity are shown in panel (c). The T/S diagrams are shown in panel  
 920 (d).

921

921



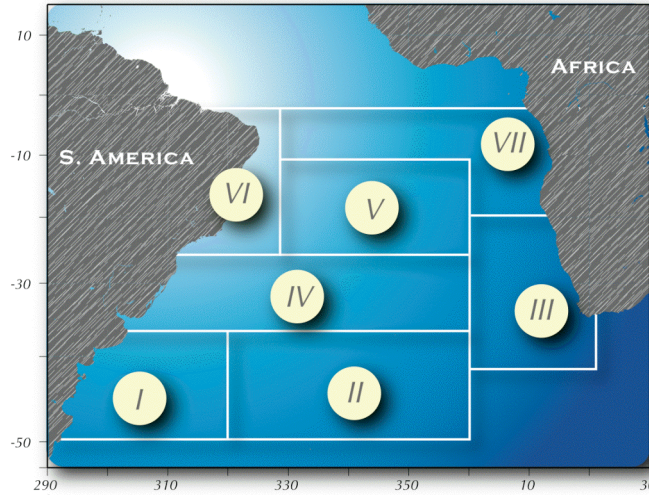
922

923

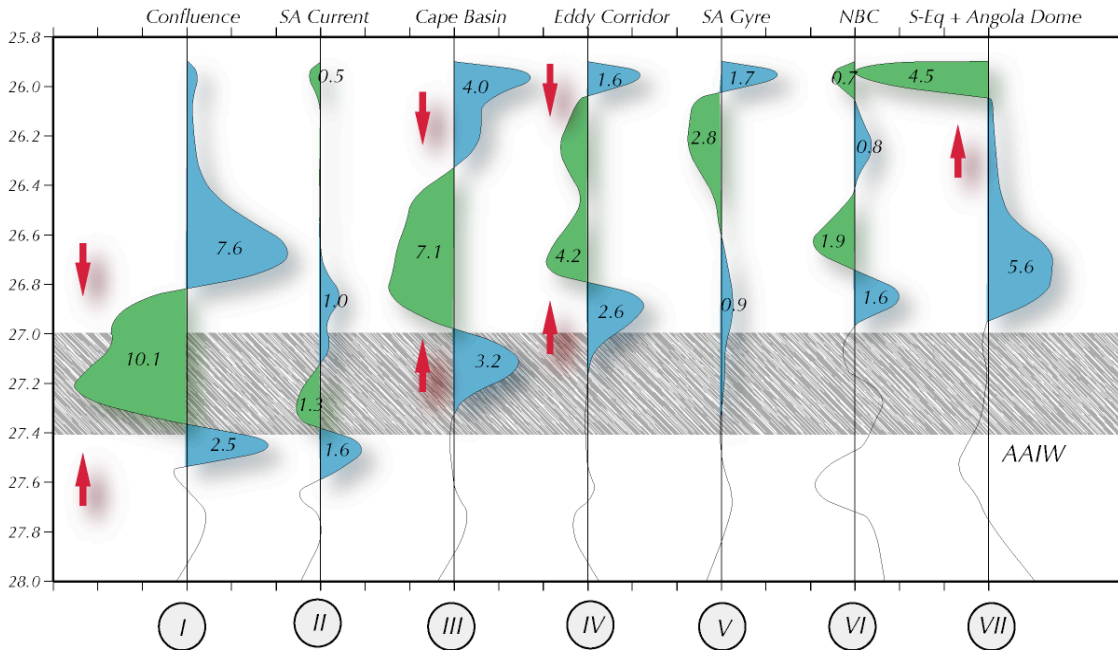
924

925 **Figure 5:** Left panel: Zonally integrated Meridional Overturning in neutral density  
926 coordinate. To indicate the position of the mixed layer, maximum surface layer density in  
927 the monthly mean field is evaluated. The dotted line shows the 10% percentile along  
928 latitude circles and can be considered a lower bound of the maximum mixed layer density  
929 at each latitude. Right panel: Model transports in isopycnal layers into the Atlantic  
930 through 30°S. The units on the horizontal axis correspond to convergence within 0.1  
931 neutral density ranges (Adapted from Schouten and Matano, 2006)

932



932

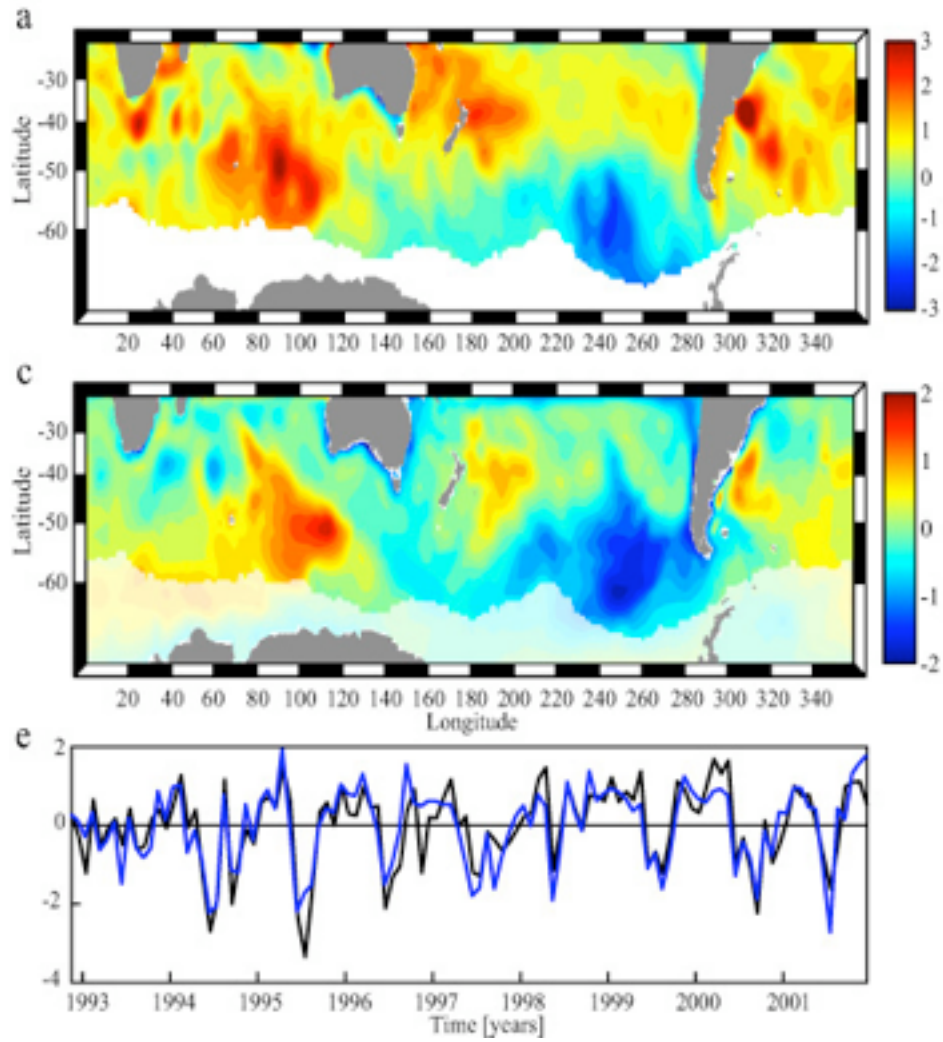


933

934

935 **Figure 6:** Water mass transformation in the South Atlantic computed from the product of  
 936 the POCM model. Top: Location of the seven boxes where volume divergences at  
 937 discrete sigma levels were computed. Bottom: sign and magnitude of the water mass  
 938 transformations.

939



939

940

941 **Figure 7:** Results of the Principal Estimator Patterns between SSH and wind stress curl.

942 Top: SSH anomalies, Middle: wind stress anomalies. Bottom: time dependence of the

943 principal mode. Blue is from the POCM and black is from the AVISO data.